The influence of wave vector dependent dielectric properties on rotational friction. Rotational diffusion of phenoxazine dyes

D. S. Alavi, R. S. Hartman, and D. H. Waldeck

Citation: The Journal of Chemical Physics **95**, 6770 (1991); doi: 10.1063/1.461788
View online: http://dx.doi.org/10.1063/1.461788
View Table of Contents: http://scitation.aip.org/content/aip/journal/jcp/95/9?ver=pdfcov
Published by the AIP Publishing

The influence of wave vector dependent dielectric properties on rotational friction. Rotational diffusion of phenoxazine dyes

D. S. Alavi,[a] R. S. Hartman, and D. H. Waldeck
Department of Chemistry, University of Pittsburgh, Pittsburgh, Pennsylvania 15260

(Received 16 April 1991; accepted 16 July 1991)

The rotational diffusion of three mechanically similar phenoxazine dyes possessing distinct electrical properties was studied in isopropanol. The results, along with previously presented results from other polar solvents, were analyzed in terms of continuum theories for rotational dielectric friction. It was found that a continuum based theory can account for the observed rotational relaxation dynamics, but only with realistic modeling of the solute charge distribution (not a point dipole), and by accounting for both frequency and wave vector dependences of the solvent dielectric properties.

INTRODUCTION

The liquid state of matter is exceedingly complex and far from completely understood. The molecules in a liquid are in intimate contact, and intermolecular interactions will be very important in determining the behavior of a liquid. Diffusion based descriptions of molecular rotation have generally been used to model the motion of medium sized (several hundred cubic angstroms) solute molecules in liquid solutions. In this diffusive regime, measurement of solute reorientation times becomes a sensitive probe of the rotational friction. In the most general case this friction will depend on both frequency and wave vector dependent solvent properties, and possibly also on the molecular characteristics of the particular solvent being studied.

How is the rotational friction modeled? A tractable approach uses continuum based theories for the solvent and models the solute properties in some specific way. The liquid is treated as a continuum characterized by its bulk properties, such as viscosity or dielectric constant. The friction experienced by the solute molecule for rotational motion is computed within this continuum. Although this treatment offers the advantage of generality, the application of bulk properties of a liquid to motions on a molecular length scale may be physically inappropriate. Consequently, such models are usually only qualitatively correct in predicting the diffusive behavior of small or medium sized solute molecules in liquid solutions. The relationship between molecular properties and the friction are not clearly understood on this length scale.

Considerable experimental and theoretical effort has been expended on the description of rotational friction for solute molecules. Reviews of this work are available.[1-3] The experimental results are often interpreted in terms of hydrodynamics. Workers[1,4] have shown that for a single solute in a single solvent the dependence of the rotational relaxation time on the solvent viscosity is given by the hydrodynamic model, if physical parameters of the system such as pressure and temperature are varied. In contrast, a wide range of observations are found when solute properties such as size, charge, and polarity are varied. Often specific molecular interactions are used to explain these observations. Noteworthy is recent progress toward understanding the effect of size and roughness of the solute on the rotational relaxation.[5,6]

An important class of interactions between solute and solvent are dielectric interactions. Dielectric friction on a rotating solute arises from the energy dissipation in a frequency dependent dielectric medium under the influence of a time varying electric field. As the solute rotates, the field of its charge distribution changes with time, and the dissipation of energy within the surrounding dielectric medium produces friction. In recent years many workers have investigated the influence of dielectric friction on medium sized molecules.[7-10] Many of these experimental studies have been performed with a single solute in a series of solvents. A more rigorous test of continuum dielectric friction theories is needed, in which solvent properties are varied by changing the temperature or pressure of a single solvent. Furthermore, all of these previous workers compare the reorientation of a charged solute with models developed for polar but neutral solutes. More thorough testing of these theories is required.

Earlier work from this laboratory has begun to address these issues.[11-15] Studies of the rotational diffusion of three phenoxazine dyes with similar structures but differing electronic properties have been performed in a variety of polar solvents over a range of temperatures. Studies of these solutes in pure dimethylsulfoxide (DMSO)[11-13] and in binary mixtures of water/DMSO and water/propanol[14] have already appeared, and it was found for pure DMSO that the dielectric friction could be accounted for by more realistically modeling the solute charge distribution.[13] The data from solvent mixtures, on the other hand, had until recently defied quantitative modeling. Reported herein are results for rotational diffusion of these solutes in isopropanol, and an extension of dielectric friction theory which is able to account for all of the data from the various solvents studied.

This paper is organized as follows. First the experimental apparatus and techniques are briefly described, along with synthesis and characterization of the samples studied.

[a] Present address: National Institute of Standards and Technology, Gaithersburg, Maryland 20899.

 0021-9606/91/216770-14$03.00

Following this, the necessary theoretical background is presented, and previously published results for rotational diffusion of phenoxazine dyes in pure DMSO[11–13] and in water/DMSO and water/propanol mixtures[14] are summarized. Next, the experimental results and analysis for rotational diffusion of these dyes in isopropanol is presented, along with further analysis of the earlier data in other solvents. The results are interpreted in terms of a generalized theory of dielectric friction, which was presented earlier[13] and is extended here. Finally, the major findings and conclusions of this work are summarized.

EXPERIMENT

Rotational diffusion measurements were performed using time resolved optically heterodyned polarization spectroscopy (OHPS), a pump/probe technique described in detail elsewhere.[12,15,16] The pump/probe apparatus was also described earlier. Briefly, the laser source consisted of a cw mode locked Nd:YAG laser which was frequency doubled and used to synchronously pump two independently tunable rhodamine 6G dye lasers, which provided the pump and probe pulses. Cross correlation measurements were used to determine the time resolution, and were typically 8–9 ps FWHM. Pump and probe beams were chopped at 1600 and 900 Hz, respectively, and the signal from the photomultiplier detected at the sum frequency (2500 Hz) by a lock-in amplifier. A microcomputer controlled the variable pathlength and stored the signal from the lock-in.

The molecules studied were three phenoxazine dyes, resorufin (anionic, sodium salt), resorufamine (neutral), and oxazine 118 (cationic, chloride salt). They were chosen because their similar structures would eliminate effects of solute size and shape on the reorientation times (Fig. 1). Their axial radii, volumes, and hydrodynamic parameters, F and C_{slip} (which are explained below), are given in Table I. The volume was computed as that of the corresponding ellipsoid using the axial radii, which were found via standard bond lengths and atomic radii.[17] The variation in volume caused by a 10% variation in the axial radii is 30%. The shape factor, F, changes by about 13% with a 10% change in the axial ratios.

The hydrodynamic friction coefficients were obtained by approximating the molecules as ellipsoids and computing the friction for rotation about each axis in the principal axis system. The slip boundary coefficients were obtained from Youngren and Acrivos.[18] The molecules were treated as ellipsoids with their transition moments along the longest of their three principal axes, so the anisotropy is, in general, a double exponential.[1] In fact, as shown earlier,[13,15] one of the two exponentials dominates the decay, and F and C_{slip} were calculated based on the friction coefficients for rotation about the two axes perpendicular to the transition moment.

Resorufin was obtained commercially (sodium salt, Aldrich) and used as received. Oxazine (chloride salt) and resorufamine were not available commercially and had to be synthesized.[19] The synthesis proceeded by nitration of phenoxazine at the 3 and 7 positions, followed by catalytic hydrogenation of the nitro groups to amino groups. Workup in aqueous HCl resulted in oxazine 118 chloride. Acid hydrolysis of the oxazine yielded resorufamine. All three dyes yielded single spots upon thin layer chromatographic analysis, and their identities were confirmed by visible[19,20] and NMR (nuclear magnetic resonance) spectra.

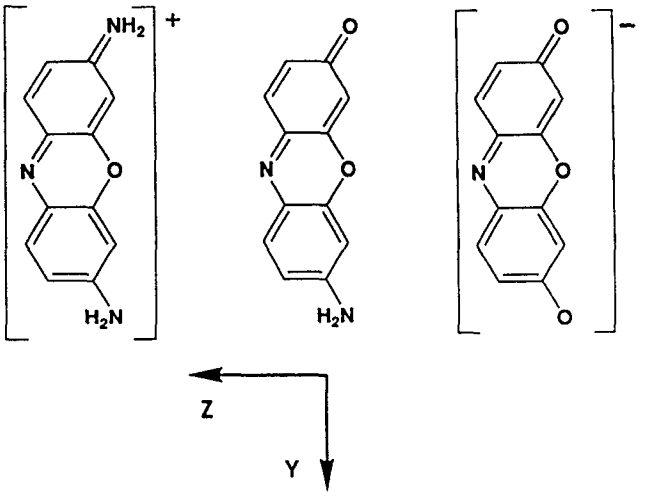

FIG. 1. Molecular structures of three phenoxazine dyes with axis system. The cation is oxazine, the anion is resorufin, and the neutral resorufamine.

The electrical properties of all three solute molecules were studied by electronic structure calculations and by steady state spectroscopy. The calculations were performed on the departmental FPS 500 computer using the GAUSSIAN 88[21] software package. First, the molecular geometries were optimized using the MNDO (modified neglect of differential overlap) algorithm, and then Hartree–Fock electronic structure calculations (STO-3G) were performed for the ground electronic state. All three molecules were restricted to be planar and the ionic dyes were constrained to have a plane of symmetry perpendicular to the molecular frame. The dipole moments were calculated by the program, in addition to the overall Mulliken charge distribution of the three solutes. The results of these calculations are summarized in Fig. 2 and Table I. Unfortunately, the GAUSSIAN 88 program is unable to properly calculate the electronic structure for singlet excited states, so excited state charge distributions could not be obtained. The ground state dipole moment and the dipole moment change upon electronic excitation were estimated from solvent induced shifts in absorption and fluorescence spectra as described elsewhere,[12,22] and are summarized in Table I.

Isopropanol (iPrOH) was chosen as a hydrogen bonding solvent with a size and shape similar to that of DMSO. The solvent was 99.9% pure (from Baker) and used as received. Temperature dependent viscosity and dielectric data were taken from the literature.[23] Rotational diffusion studies were performed for resorufamine, resorufin and oxazine (both ground and excited states) in iPrOH over a range of temperatures from 275 to 330 K using the OHPS technique. For the excited state experiments the measured decays could be fit by a single exponential (nonweighted least squares fit). For the ground state measurements the decays could not be completely described by a single exponential, but required two exponentials. The correlation times for the two expo-

TABLE I. Solute properties.

Solute	Axial radii (Å)	V (Å^3)	F	C	$q(e)$	μ_G(D) Spec	μ_G(D) Calc	$\Delta\mu$(D) Spec
Resorufin	6.5×3.5×2.0	190	2.32	0.25	−1	3.3	2.6(z)	1.5
Resorufamine	6.5×3.5×2.0	190	2.32	0.25	0	3.2	5.6(y)	3.8
Oxazine	6.5×3.5×2.0	190	2.32	0.25	+1	3.7	−2.0(z)	2.4

nential fits were virtually identical to the decay times from the corresponding one exponential fits. The excited state population decay, was measured using time correlated single photon counting and found to be a single exponential. The resulting decay times, τ_F, were used to calculate τ_{OR} (correlation time for the ground state, single exponential for the excited state) and τ_{OR1} and τ_{OR2} (double exponential, ground state). The time constant τ_{OR} was used in the analysis presented here and the values are reported in Table II. The source and significance of the multiexponential decays is presently under investigation.

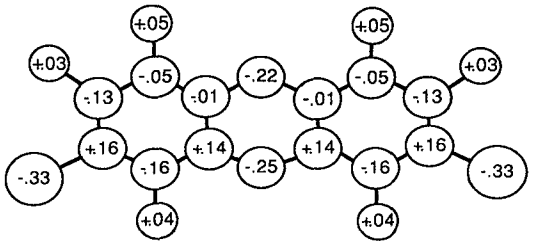

RESORUFIN

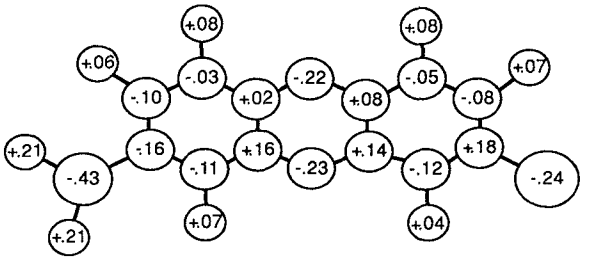

RESORUFAMINE

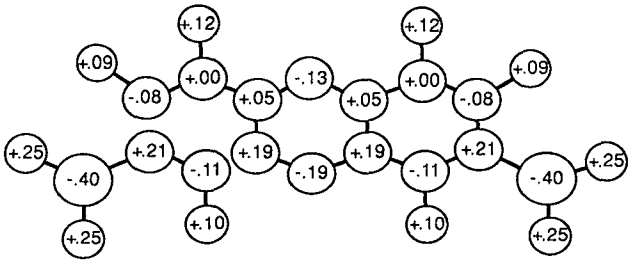

OXAZINE

FIG. 2. Charge distributions calculated by the GAUSSIAN 88 program.

FRICTION MODELS

As shown earlier,[13,15] for a molecule with its transition moment along the principal axis about which the friction is much smaller than the other two, the correlation function $r(t)$ approximates a single exponential with decay time $\tau_{OR} \approx \bar{\zeta}/6kT$, where $\bar{\zeta}$ is the average friction about the two axes perpendicular to the transition moment. This friction is decomposed into a mechanical contribution, modeled by hydrodynamics, and a dielectric contribution, modeled by different continuum theories.

Hydrodynamic friction

The mechanical contribution is modeled using the Debye–Stokes–Einstein (DSE) theory, which treats the solute as a smooth ellipsoid rotating in a continuum fluid and solves a linearized Navier–Stokes hydrodynamic equation (assuming slow, steady motion of the solute) to calculate the mechanical friction.[1,3,5,18,24–27] This leads to the prediction that the reorientation time, τ_{OR}, should be proportional to the solvent viscosity divided by absolute temperature, η/T. More specifically,

$$\tau_{OR} = \frac{V\eta}{kT} FC, \tag{1}$$

where V is the solute molecular volume, k is the Boltzmann constant, F is a parameter which accounts for the solute shape (axial ratios), and C is a parameter which is determined by both the shape and boundary condition assumed in the hydrodynamic calculation of the friction. It is through these two parameters that the continuum theory accounts for the intermolecular potential between the solute and the solvent molecules.

TABLE II. Experimental rotational relaxation times in isopropanol.

	Resorufin (τ_{OR} (ps) ± 5%)		Resorufamine (τ_{OR} (ps) ± 5%)		Oxazine (τ_{OR} (ps) ± 5%)		
T (K)	S_0	S_1	S_0	S_1	S_0	S_1	η (cP)
276	595	875	529	1079	960	1139	4.07
280	···	···	···	822	···	···	3.56
285	432	641	400	606	734	869	3.03
294	374	432	···	···	483	637	2.29
300	···	···	268	446	···	···	1.92
305	262	291	···	···	307	455	1.66
315	···	···	150	311	···	···	1.27
320	157	180	···	···	211	266	1.11
330	···	···	119	163	···	···	0.871
334	105	127	···	···	141	173	0.793

The boundary condition used in the calculation of the hydrodynamic friction ranges from "slip" to "stick." The stick boundary condition requires zero relative velocity between the surface of an object and the first layer of solvent. This boundary condition is appropriate for macroscopic objects and macromolecules. The slip boundary condition is so named because it specifies that the solvent can exert no tangential stress on an object. This boundary condition is considered appropriate for small to medium sized molecules in nonpolar, noninteracting solvents. The value of F ranges from one for a sphere to larger values as the shape becomes less spherical. For the stick boundary condition and any molecular shape, the value of C is one. But for the slip boundary condition, C ranges from zero for a sphere to some value $C_{\text{slip}} < 1$ for a nonspherical particle. Extensive tabulations of the friction coefficients for both slip[18,26] and stick[27] are available, greatly simplifying the calculation of F and C_{slip} for a given solute.

Recent theoretical and experimental work has shown that the use of a slip boundary condition in conjunction with a molecular shape that is rough, or bumpy (i.e., not a smooth ellipsoid), results in a friction coefficient which approaches the stick value for the corresponding smooth shape as the size and roughness increase.[5] The amount of roughness and the relative solute to solvent size required to proceed from the slip to stick limits are still not resolved.[6] Some theoretical work has also appeared which attempts to relate the intermolecular potential to the boundary condition.[28]

Dielectric friction

A variety of treatments of dielectric friction are available.[22,29-31] Of these, three types will be discussed here. First are the models of Nee and Zwanzig[29] and Hubbard and Wolynes,[30] which treat the solvent as a dielectric continuum and model the solute as a spherical cavity containing a point dipole. Second is a semiempirical approach to the dielectric friction, in which van der Zwan and Hynes[22] have shown how the fluorescence Stokes shift of the solute in the solvent of interest is related to the dielectric friction. Third is a model presented by Alavi and Waldeck,[13] which is analogous to the Nee–Zwanzig model, but extended to an arbitrary charge distribution in the cavity. Although molecular models of dielectric friction are available,[32] they have either been applied to translational motion and require some knowledge of the intermolecular potential or require unavailable properties of the solvent. Comparisons with such models may be possible in the future. Continuum theories offer the advantages of simplicity and the calculation of molecular friction in terms of easily accessible bulk solvent properties.

For a dipolar solute the Nee–Zwanzig (NZ) theory[29] yields a frequency dependent friction coefficient by calculating the torque exerted on a point dipole rotating at the center of a spherical cavity in a continuous dielectric. For any charge distribution in such a cavity, the field of the charge distribution polarizes the surrounding dielectric and induces a polarization charge density at the cavity boundary. This polarization charge density in turn produces a field within the cavity called the reaction field. The torque arises because the direction of the dipole's reaction field lags behind the rotating dipole's orientation as a result of the frequency dependence of the dielectric constant. The friction coefficient is calculated in the limit of zero frequency for a medium exhibiting Debye (single exponential) dielectric relaxation behavior. If one assumes the mechanical and dielectric components of the friction are separable, this treatment leads to the following expression for the reorientation time of a solute molecule with dipole moment μ:

$$\tau_{OR} = \tau_{\text{HYD}} + \frac{\mu^2}{kTa^3}\frac{(\epsilon_S - 1)}{(2\epsilon_S + 1)^2}\tau_D, \tag{2}$$

where a is the radius of the cavity in the dielectric occupied by the solute molecule, ϵ_S is the static dielectric constant, τ_D is the Debye relaxation time, T is the temperature, and μ is the dipole moment of the solute in vacuum. In this expression the dielectric constant of the cavity is taken to be one.

More recently, Hubbard and Wolynes[30] employed a different method to calculate the friction. Their concern was that in Eq. (2) the reorientation time becomes infinitely long as $\tau_D \to \infty$, whereas in reality the solute molecule should have a finite reorientation time even in the presence of a fixed field. They remedied this situation by solving a rotational Smoluchowski equation with fluctuating torques to yield an expression for the dipole correlation function. In the limit that the torques from the polarization of the dielectric fluctuate much more rapidly than the dipole reorients, the Nee–Zwanzig expression is obtained. This regime is appropriate for some of the experimental studies presented previously.[11,12] In the case where the torque fluctuations are long lived, the Hubbard–Wolynes model predicts nonexponential behavior for the dipole correlation function. This is the appropriate limit for the experimental studies which will be discussed here.

It should also be noted that while the concern of Hubbard and Wolynes regarding the use of Eq. (2) when τ_D is large is justified, it does not mean that the Nee–Zwanzig model is necessarily incorrect. Equation (2) was obtained in the limit of zero frequency, assuming the molecular reorientation is slow compared to the dielectric relaxation. If this time scale separation does not hold, the full frequency dependent form of Eq. (2) can be used to yield a frequency dependent diffusion constant. Solution of the rotational diffusion equation with a frequency dependent friction coefficient leads to nonexponential decay of the dipole correlation function, and also averts the problem of long reorientation times as τ_D becomes large.

The semiempirical model of van der Zwan and Hynes (ZH)[22] relates the dielectric friction experienced by a solute in a solvent to the correlation time for solvation, τ_S, and the solute Stokes shift, S, in the solvent. S is given as $h\nu_A - h\nu_F$, where $h\nu_A$ is the energy of the zero–zero transition for absorption and $h\nu_F$ is the energy of the zero–zero transition for fluorescence. The Stokes shift gauges the magnitude of the solute/solvent coupling, while the solvation time is a measure of the lag between the solute orientation and the solvent polarization. Their result is

$$\zeta_D(\Delta\mu)^2 = S\tau_S, \tag{3}$$

where $\Delta\mu$ is the change in dipole moment upon electronic

excitation. Numerous studies of solvation dynamics[33] indicate that the solvation time τ_S is approximately given by the solvent longitudinal relaxation time $\tau_L = \tau_D(\epsilon_\infty/\epsilon_S)$ and is relatively independent of the solute properties. This relationship holds to within a factor of 2 or 3, despite the fact that the model which predicts τ_L for the characteristic solvation time also predicts single exponential relaxation for the solvent response, whereas the observed dynamics are nonexponential. The expression for the dielectric friction in electronic state i is given by

$$\zeta_D(\mu_i) = \left(\frac{\mu_i}{\Delta\mu}\right)^2 S\tau_S, \tag{4}$$

which is just a rescaling of Eq. (3) from a dipole strength of $\Delta\mu$ to one of μ_i. Assuming separable mechanical and dielectric friction components, the rotation time is given by

$$\tau_{OR} = \tau_{\mathrm{HYD}} + \frac{1}{6kT}\left(\frac{\mu}{\Delta\mu}\right)^2 S\tau_S. \tag{5}$$

A more physically realistic model for rotational dielectric friction was put forth by Alavi and Waldeck.[13] The physical basis of the model is the same as the Nee–Zwanzig theory, but the computation was performed for an arbitrary distribution of point charges in the cavity. This model treats the charge distribution of a solute molecule more reasonably and eliminates the ambiguity involved in assigning a dipole moment to a charged solute. For polar solvents the expression for the friction about the z axis for a solute rotating within a spherical cavity in a Debye medium in the limit of zero frequency is

$$\begin{aligned}\zeta_D = {} & \frac{8}{a}\frac{(\epsilon_S-1)}{(2\epsilon_S+1)^2}\tau_D \sum_{j=1}^{N}\sum_{i=1}^{N}\sum_{L=1}^{\infty}\sum_{M=1}^{L}\left(\frac{2L+1}{L+1}\right) \\ & \times\frac{(L-M)!}{(L+M)!}M^3 q_i q_j \left(\frac{r_i}{a}\right)^L\left(\frac{r_j}{a}\right)^L P_L^M(\cos\theta_i) \\ & \times P_L^M(\cos\theta_j)\cos M\phi_{ji}.\end{aligned} \tag{6}$$

Here the charge q_i is located at spherical coordinates r_i, θ_i, and ϕ_i, $\phi_{ji} \equiv \phi_j - \phi_i$, the cavity radius is a, and the $P_L^M(x)$ are the associated Legendre functions. This expression for the friction has the same dependence on the dielectric properties of the solvent as the Nee–Zwanzig expression for a point dipole, but a very different dependence on the electrical properties of the solute. In fact, while the $L = 1$ term in Eq. (6) is nearly the same as the Nee–Zwanzig result (with μ^2 replaced by $\mu_x^2 + \mu_y^2$, assuming rotation about the z axis), the higher order terms neglected by the assumption of a point dipole can be quite significant, and cannot, in general, be neglected.

As noted in the original presentation of the dielectric friction theory for a charge distribution,[13,15] the expression for the friction becomes extremely sensitive to the cavity radius as charges are brought closer to the cavity boundary. This sensitivity was interpreted as possible evidence that application of a continuum theory may be inappropriate on molecular length scales. As charges are brought close to the boundary, terms in the reaction potential with large L become more important. The potential from these terms varies over progressively smaller length scales, and eventually the solvent will not be able to respond to the field from the charge distribution. The use of a dielectric constant which depends on both frequency and wave vector is one way such solvent size effects might be incorporated into a continuum dielectric friction theory. This work describes a simple way of incorporating this wave vector dependence into the dielectric friction theory. In the original calculation of the static reaction field one replaces the static dielectric constant ϵ_S by a dielectric constant which depends on the index L, $\epsilon_S(L)$. The form chosen for $\epsilon_S(L)$ has $\epsilon_S(L) = \epsilon_S$ for $L \leqslant L_{\max}$ and $\epsilon_S(L) = 1$ for $L > L_{\max}$. This form for $\epsilon_S(L)$ results in truncation of the series in Eq. (6) at $L = L_{\max}$, and eliminates some of the sensitivity of the calculated friction to the cavity radius chosen. For unassociated molecular liquids, $L_{\max}$ could be chosen so that the average area of a sector between the nodes of a spherical harmonic at the cavity boundary would be greater than the cross sectional area of one solvent molecule. For associated liquids such as the alcohols, the appropriate length scale criterion for choosing $L_{\max}$ may not be the size of a single molecule, but rather the size of complexes of many solvent molecules whose dynamics dominate the solvent's dielectric relaxation behavior (see below).

While this functional form for the dielectric constant simplifies the analysis and will be shown to capture the essential features of the solute rotational dynamics, it remains a crude model. The relationship between the wave vector k and the parameter $L_{\max}$ is not clear. A continuous decrease of ϵ with increasing wave vector would be more realistic than the step function assumed here. The choice of $L_{\max}$ and its interpretation in terms of microscopic solvent structure is ambiguous, although it seems clear that an inverse relationship exists between $L_{\max}$ and the characteristic length scale of solvent structure. In the analysis which follows $L_{\max}$ is chosen to yield agreement between the theory and experiment, and the resulting value of $L_{\max}$ is interpreted in light of previous knowledge concerning the solvent structure.

All of the theories discussed above yield expressions of the form

$$\tau_{OR} - \tau_{\mathrm{HYD}} = P\frac{(\epsilon_S-1)\tau_D}{(2\epsilon_S+1)^2 T}, \tag{7}$$

where

$$P = P_{\mathrm{NZ}} = \frac{\mu_{\mathrm{NZ}}^2}{ka^3} \tag{8}$$

for the Nee–Zwanzig theory,

$$P = P_{\mathrm{ZH}} = \frac{2\mu_{\mathrm{ZH}}^2\epsilon_\infty S}{3k(\Delta\mu)^2} \tag{9}$$

for the van der Zwan–Hynes theory (where the solvation time τ_S is modeled as τ_L and $(\epsilon_S - 1)/(2\epsilon_S + 1)^2 \approx 1/4\epsilon_S$, a reasonable approximation when $\epsilon_s \geqslant 10$), and

$$\begin{aligned}P = {} & P_{\mathrm{CD}} \\ = {} & \frac{4}{3ka}\sum_{j=1}^{N}\sum_{i=1}^{N}\sum_{L=1}^{L_{\mathrm{MAX}}}\sum_{M=1}^{L}\left(\frac{2L+1}{L+1}\right)\frac{(L-M)!}{(L+M)!}M^3 \\ & \times q_i q_j\left(\frac{r_i}{a}\right)^L\left(\frac{r_j}{a}\right)^L P_L^M(\cos\theta_i) \\ & \times P_L^M(\cos\theta_j)\cos M\phi_{ji}\end{aligned} \tag{10}$$

for the charge distribution theory (CD). While the slope P_{NZ} depends only on solute properties (μ and a), P_{ZH} and P_{CD} depend on both solute and solvent properties. P_{ZH} depends on ϵ_∞ (solvent), μ and $\Delta\mu$ (solute), and S (both). P_{CD} depends on the solute charge distribution and radius a, as well as the wave vector dependence of the solvent dielectric constant (through L_{max}).

PREVIOUS EXPERIMENTAL RESULTS

Experimental results have already been reported for rotational diffusion of these phenoxazine dyes in pure DMSO,[11-13] and for oxazine in water/DMSO and water/*n*-propanol binary mixtures,[14] all as functions of temperature. The analysis of this data in terms of dielectric friction models is given in Table III and was performed as follows. After measurement of τ_{OR} and calculation of τ_{HYD} using slip hydrodynamics, the quantity $\tau_{OR} - \tau_{SLIP}$ was plotted vs $(\epsilon_s - 1)\tau_D/[(2\epsilon_s + 1)^2 T]$, and the slope was obtained from a weighted least squares fit. For the point dipole theories, this slope was used to calculate *effective* dipole moments for the solute using Eqs. (8) and (9). For the Nee–Zwanzig model a cavity radius of 3.6 Å was assumed (chosen to yield the molecular volume of 190 Å^3). For the charge distribution theory, the Mulliken charge distributions obtained from GAUSSIAN 88 were used in Eq. (10), and L_{max} made large enough to assure convergence of the series ($L_{max} = 30$ was sufficient). The cavity radius was adjusted to obtain agreement between the experimental slope and Eq. (10) for each of the three solutes in DMSO.

Two important features of these data stand out. First, in all cases the point dipole dielectric friction theories significantly overestimate the solute dipole moments, indicating that they severely underestimate the dielectric friction. In many cases the dielectric friction is underestimated by more than 2 orders of magnitude. Second, the charge distribution dielectric friction expression (without accounting for wave vector dependence of the dielectric constant) yields reasonable agreement with the experimental data for pure DMSO. However, the data from the solvent mixtures clearly are not adequately accounted for by either theory. Where the point dipole theories underestimate the friction, the charge distribution theory seems to overestimate it. These results and the experimental results from rotational diffusion studies of these dyes in isopropanol presented here will be analyzed further in terms of the wave vector dependent dielectric friction theory described above.

PHENOXAZINES IN ISOPROPANOL

Hydrodynamics

DSE plots of τ_{OR} vs η/T for resorufamine, resorufin, and oxazine in isopropanol are shown in Fig. 3, along with calculated lines for slip and stick boundary conditions. The results of fitting these points to straight lines (weighted least squares) are given in Table IV. The ground state slope of resorufamine is fairly close to (but above) the stick prediction, while the excited state slope is about a factor of two larger. For resorufin the ground state slope exceeds the stick slope by about 25%, and the excited state slope exceeds the stick prediction by almost a factor of 2. The ground state oxazine slope is a factor of 2 larger than the stick slope, while the excited state slope is 2½ times larger. One immediately striking feature is the change in order of the three solutes

TABLE III. Summary of rotational diffusion data for phenoxazine dyes in DMSO, *n*-propanol/water and DMSO/water.

Solute	Solvent	Measured[c] slope (10^4 K)	μ_{NZ} (D)[d]	μ_{ZH} (D)[e]	Calculated slope (10^4 K) Eq. (10), all L	Cavity radius (Å)
Resorufin (S_0)[a]	DMSO	10.9	26	18	11.4	6.75
Resorufamine (S_0)[a]	DMSO	31.1	44	19	31.2	6.50
Oxazine (S_0)[a]	DMSO	67.6	65	36	67.7	6.70
Oxazine (S_1)[a,b]	DMSO	76.5	70	84	···	···
Oxazine (S_1)[b]	0.6/0.4 DMSO/water	38.8	50	42	···	···
Oxazine (S_1)[b]	0.32/0.68 DMSO/water	30.6	44	38	···	···
Oxazine (S_1)[b]	water	49.5	56	36	···	···
Oxazine (S_1)[b]	0.2/0.8 PrOH/water[f]	26.9	42	38	···	···
Oxazine (S_1)[b]	0.5/0.5 PrOH/water	10.6	26	24	···	···
Oxazine (S_1)[b]	PrOH	2.4	13	12	···	···

[a] From Refs. 11–13.
[b] From Ref. 14.
[c] Effective dipole moment obtained using Eq. (8); cavity radius used was 3.6 Å.
[d] Effective dipole moment obtained using Eq. (9).
[e] Slopes are from fits of $\tau_{OR} - \tau_{SLIP}$ vs $(\epsilon_s - 1)\tau_D/(2\epsilon_s + 1)^2 T$.
[f] Note: PrOH is *n*-propanol.

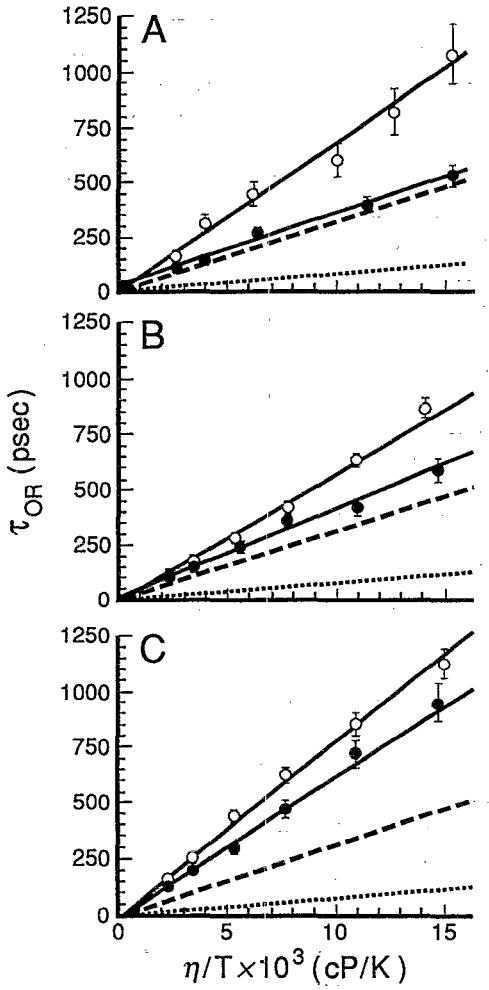

FIG. 3. Plots of τ_{OR} vs η/T in isopropanol. (A) resorufamine, (B) resorufin, (C) oxazine. Open symbols are excited state data points and closed symbols are ground state data points. The long dashed line is the stick prediction and the short dashed line is the slip prediction.

compared to their ordering in DMSO. In DMSO resorufin reorients fastest and oxazine slowest,[11–13] whereas in isopropanol resorufamine reorients fastest (in the ground state).

Hydrodynamics alone cannot explain these results. The very strong state dependence of the reorientation times indicates that the coupling between the solute and solvent is much stronger in the excited state, particularly for resorufamine. This is not so surprising, since resorufamine has a relatively large increase in dipole moment upon electronic excitation, a large Stokes shift, and exhibits state dependent rotation behavior in DMSO.[11,12] The state dependent behaviors of resorufin and oxazine are not as dramatic, but are no doubt related to the differing electronic properties of the solutes in their excited states. This behavior will be discussed further later. The intercepts for all six lines lie fairly close to zero as predicted by the simple DSE model.

It was empirically found that the viscosity can be fit to an Arrhenius form, $\eta = \eta_0 \exp(E_\eta/\mathrm{RT})$. Substitution of this form into the DSE expression [Eq. (1)] shows that the slope of a plot of $\ln(\tau_{OR} T)$ vs $1/T$ should yield an activation energy of E_η. The values for E_{OR} thus obtained are also

TABLE IV. Debye–Stokes–Einstein fitting parameters (τ_{OR} vs η/T, see Fig. 3).

Solute	Slope (ns K/cP)	Intercept (ps)	$\Delta\tau/\tau$ [a]	E_{OR} [b] (kcal/mol)
Resorufin (S_0)	41.4 ± 1.9	11.0 ± 8.3	0.08	4.8
Resorufin (S_1)	59.4 ± 1.6	-19.2 ± 6.5	0.05	5.7
Resorufamine (S_0)	33.8 ± 2.3	24.6 ± 10.6	0.09	4.5
Resorufamine (S_1)	68.1 ± 4.2	-6.2 ± 20.3	0.12	5.2
Oxazine (S_0)	63.6 ± 2.9	-10.5 ± 12.0	0.08	5.5
Oxazine (S_1)	80.8 ± 2.5	-14.5 ± 10.5	0.06	5.3
Slip	8.0	0.0	···	5.2
Stick	31.9	0.0	···	5.2

[a] This ratio provides a measure of the error in rotational relaxation times.
[b] Activation energy for rotational motion, see the text for details.

given in Table IV, and are in reasonable agreement with $E_\eta = 5.2$ kcal/mol for isopropanol.

Some of these molecules have been studied previously in alcohols, namely oxazine and resorufin at room temperature.[4(e),9(c),10] The decay times observed here are in reasonable agreement with previous results, although the studies of Blanchard did not find as dramatic a state dependence for the reorientation of resorufin in the butanols as found here in isopropanol.

Point source dielectric friction

We attempted to account for the observed reorientation behavior of these dyes in isopropanol using the Nee–Zwanzig dielectric friction expression [Eq. (2)]. The plots of $\tau_{OR} - \tau_{\mathrm{slip}}$ vs $(\epsilon_S - 1)\tau_D/(2\epsilon_S + 1)^2 T$ are shown in Fig. 4 and the fitting parameters are given in Table V. While this expression qualitatively explains the trends in the data, the quantitative comparison is poor. The dipole moments calculated from the slopes using Eq. (8), assuming a mean cavity radius of 3.6 Å, are also given in Table V. These dipole moments are not as large as those calculated from the DMSO data, but are all a factor of 2 or more larger than the estimates in Table I. Setting the ground state moments equal to the values calculated by the GAUSSIAN 88 program and using the difference in slopes yields excited state moments of 12.9, 8.3, and 8.6 D for resorufamine, resorufin, and oxazine, respectively. These values still seem too large, but again, not nearly as large as those calculated for DMSO. As with the polar aprotic solvent DMSO, the Nee–Zwanzig expression underestimates the rotational dielectric friction for these phenoxazine dyes in the hydrogen bonded solvent isopropanol. This comparison to DMSO is particularly noteworthy since it has been argued[4(c)] that proper treatment of long range dielectric friction effects is necessary in order to evaluate the influence of more localized, specific solute/solvent interactions, such as hydrogen bonding, on the friction. Based on this assertion one would think these dielectric friction theories should work better in a polar

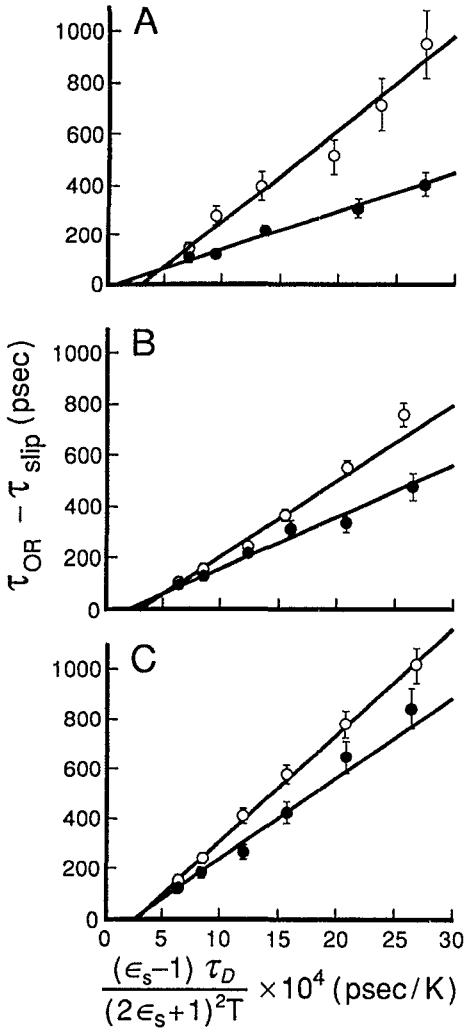

FIG. 4. Plots of $\tau_{OR} - \tau_{slip}$ vs $(\epsilon_S - 1)\tau_D/[(2\epsilon_S + 1)^2 T]$ in isopropanol. (A) resorufamine, (B) resorufin, (C) oxazine. Open symbols are excited state data points and closed symbols are ground state data points.

aprotic solvent. In contrast, the experimental data shows better (although still poor) agreement between the dielectric friction theory and experiment for the hydrogen bonded solvent than for the aprotic solvent. Clearly point source theories for dielectric friction are not adequate for quantitative modeling of this rotational diffusion data.

Semiempirical dielectric friction

The Stokes shift energy and solvation time can be used to gauge the magnitude of the dielectric friction for the solute molecules in isopropanol. As discussed earlier, this semiempirical approach should include any specific solute/solvent interactions in an effective way. The Stokes shifts for these three solutes in isopropanol are 550 cm^{-1} for resorufin, 1153 cm^{-1} for resorufamine, and 442 cm^{-1} for oxazine. The solvation time τ_S for isopropanol was approximated by the longitudinal relaxation time, $\tau_L = \tau_D(\epsilon_\infty/\epsilon_S)$, since solvation time data were not available. The Stokes shift was assumed independent of temperature. With these assumptions, the slopes from Table V can be used with the

TABLE V. Fitting parameters and dipole moments for plots of $\tau_{OR} - \tau_{SLIP}$ vs $(\epsilon_s - 1)\tau_D/[(2\epsilon_s + 1)^2 T]$ (Fig. 4).

Solute	Slope (10^4 K)	Intercept (ps)	μ_{NZ} (D)[a]	μ_{ZH} (D)[b]
Resorufin (S_0)	2.00 ± 0.11	-42 ± 11	11.3	6.5
Resorufin (S_1)	2.96 ± 0.09	-92 ± 9	13.8	8.0
Resorufamine (S_0)	1.54 ± 0.14	-16 ± 14	10.0	16.9
Resorufamine (S_1)	3.62 ± 0.25	-105 ± 26	15.3	20.7
Oxazine (S_0)	3.22 ± 0.17	-90 ± 16	14.4	15.0
Oxazine (S_1)	4.31 ± 0.15	-126 ± 14	16.7	17.5

[a] Effective dipole moments obtained using Eq. (8) with 3.6 Å cavity radius.
[b] Effective dipole moments obtained using Eq. (9).

Stokes shift and $\Delta\mu$ to find the dipole moments using Eq. (9), which are also listed in Table V. The dipole moments are larger than the estimated values, but not as large as those found from the DMSO data. However, the van der Zwan–Hynes model underestimates the dielectric friction.

Extended source dielectric friction

The dielectric friction expression for an arbitrary charge distribution rotating within a spherical cavity [Eq. (10)] was applied to the ground state rotational diffusion of these three phenoxazine dyes in isopropanol. The calculation was performed with the partial charges localized on each atomic center shown in Fig. 2, and using the same cavity radii determined for DMSO (Table III). The large difference in slopes for these dyes between DMSO and isopropanol can only be accounted for by using the charge distribution dielectric friction theory and including a wave vector dependent dielectric constant. This behavior is consistent with the fundamentally different physical processes responsible for the dielectric behavior of isopropanol as opposed to DMSO.

DMSO, a polar aprotic solvent, has a lesser degree of formation of multimolecular complexes than do the alcohols. It is likely that the dielectric relaxation occurs primarily through the reorientation of individual dipolar molecules in the liquid [Fig. 5(a)],[34] so the dielectric relaxation is rapid and described by a single relaxation time ($\tau_D \sim 20$ ps at room temperature). The dielectric friction theory was applied to the DMSO data by choosing a cutoff for the sum over L in the following manner. For a given L, the cavity boundary is divided into approximately $2L$ sectors, which will have an average area of $4\pi(a + r_{solv})^2/2L$. This area is required to be larger than the cross sectional area of a solvent molecule, πr_{solv}^2. Van der Waals radii yielded a volume of 74 $Å^3$ and a mean radius $r_{solv} = 2.6$ Å for DMSO,[17] and $a = 6.5$ Å, corresponding to the largest semiaxis of the hydrodynamic ellipsoid used to model the solutes. This procedure yielded $L_{max} = 25$ for use in the friction calculations and produced friction coefficients virtually identical to those obtained with the sum over all L. This agreement is found because the sum converges before $L = 25$. The wave vector dependent

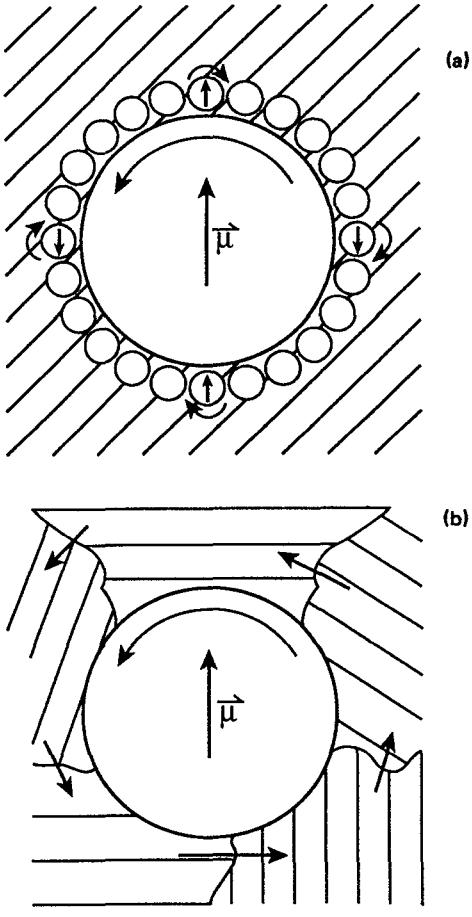

FIG. 5. Schematic drawings showing dielectric relaxation of solvent around a rotating solute. In DMSO (a), individual dipolar solvent molecules relax around the solute. In isopropanol (b), microscopic "domain" boundaries migrate around the solute.

theory is consistent with the DMSO analysis reported previously.[11-13]

In liquid alcohols nearly all of the solvent molecules are part of hydrogen bonded chains, and the dynamics of these multimolecular complexes dominates the dielectric behavior of alcohols.[23(c),34,35] One manifestation of this structure is three characteristic dispersion regions in the complex dielectric constant $\epsilon(\omega)$ of liquid alcohols, with three corresponding relaxation times. The highest frequency dispersion region corresponds to a relaxation time on the order of a few picoseconds (1.96 ps for iPrOH at 25 °C) and is believed to arise from internal rotation of the hydroxyl group within an alcohol molecule. The second region's relaxation time is typically 5–20 ps (14.5 ps for iPrOH) and its dependence on solvent size is consistent with the reorientation of single molecules. The third and dominant dispersion region is characterized by much longer relaxation times, usually several hundred picoseconds (359 ps for iPrOH). The longest relaxation time was used in all the analyses presented here. This third region represents the largest component of the relaxation process, and is believed to arise from the dissociation and/or formation of hydrogen bonds of an individual molecule with the hydrogen bonded complex which causes a net change in the dipolar moment of the complex. The rate limiting step in this scheme is the rate of bond breaking and formation. The dielectric behavior of liquid alcohols might be thought of in terms of transient microscopic "domains" made up of hydrogen bonded complexes of many alcohol molecules (molecular dynamics simulations have found average chain lengths of 15 molecules for liquid methanol at room temperature[36]). These domains would have a characteristic dipole moment whose magnitude and orientation evolves in time through this hydrogen bond making and breaking process. The bulk of the dielectric relaxation occurs not through motions of individual molecules, but through the evolution of these domains [Fig. 5(b)].

It is this change in length scale for the dielectric relaxation of alcohols, compared to DMSO, which the L dependence in ϵ tries to capture. Using the cavity radius already determined from the DMSO data, the dielectric friction coefficient [using Eq. (10)] is calculated as a function of $L_{\max}$. The numerical results are given in Table VI and show that for all three ground state molecules in isopropanol, termination of the series at $L = 3$ and $L = 4$ nearly bracket the experimental slopes in Table VI. Exact agreement for a given $L_{\max}$ is unlikely, since the friction calculated for a given molecule as a function of $L_{\max}$ does not vary continuously. This maximum L is an indicator of the average size of the fluctuating domains surrounding the solute molecule. Smaller $L_{\max}$ values correspond to larger domains, although it is not clear precisely how the domain size would be related to L when L is small. The simple approach used to arrive at $L = 25$ for DMSO is probably inappropriate for this case where the multimolecular complexes are nearly as large as, or perhaps larger than, the solute. The form for the wave vector dependent dielectric constant chosen seems to reproduce the essential features of the rotational relaxation behavior of these three phenoxazine dyes in isopropanol, including the inversion of the order of resorufin and resorufamine when compared to their order in DMSO.

The L dependent theory also explains why the point dipole dielectric friction theories seem to work better in isopropanol than in DMSO. This modeling allows the series in Eq. (10) to be cut off at a much smaller $L_{\max}$ for isopropanol than for DMSO. The $L = 1$ term is equivalent to the point dipole expression given in Eq. (2) and each additional term in the series increases the discrepancy between the two expressions. The discrepancy between the point dipole and general charge distribution expressions will be much larger for DMSO (25 terms) than for isopropanol (3–4 terms). The improvement of the point dipole approximation in isopropanol over DMSO arises from the isopropanol solvent structure which is reflected in the domain size for dielectric relaxation and the long dielectric relaxation time.

One issue not addressed by this analysis is the state dependence of the rotational diffusion of these phenoxazine dyes in isopropanol. An important extension of the work presented here would be the calculation of excited state charge distributions, so that similar calculations could be performed to try to account for the excited state reorientation times. In order to account for slower reorientation

TABLE VI. Measured and calculated slopes and L_{max} for all solvents.

Solute	Solvent	Measured slope (10^4 K)[d]	Calculated slope (10^4 K) Eq. (10)	L_{max}	Radius (Å)
Resorufin (S_0)[a]	DMSO	10.9	11.4	25	6.75
Resorufamine (S_0)[a]	DMSO	31.1	31.2	25	6.50
Oxazine (S_0)[a]	DMSO	67.6	67.7	25	6.70
Resorufin (S_0)[b]	iPrOH[e]	1.99	2.14	3	6.75
Resorufamine (S_0)[b]	iPrOH	1.54	0.81 1.91	3 4	6.50
Oxazine (S_0)[b]	iPrOH	3.22	2.37 6.13	3 4	6.70
Oxazine (S_1)[c]	*n*PrOH	2.43	2.37 6.10	3 4	6.70
Oxazine (S_1)[c]	0.5/0.5 *n*PrOH/water	10.6	6.9 11.9	5 6	6.70
Oxazine (S_1)[c]	0.2/0.8 *n*PrOH/water	26.9	26.4 32.7	11 12	6.70
Oxazine (S_1)[c]	Water	49.5	48.1 52.1	16 17	6.70
Oxazine (S_1)[c]	0.32/0.68 DMSO/water	30.6	26.4 32.7	11 12	6.70
Oxazine (S_1)[c]	0.6/0.4 DMSO/water	38.8	34.8 40.6	13 14	6.70
Oxazine (S_1)[a,c]	DMSO	76.5	67.6	25	6.70

[a] References 11–13.
[b] This work.
[c] Reference 14.
[d] Slopes are from fits of $\tau_{OR} - \tau_{SLIP}$ vs $(\epsilon_s - 1)\tau_D/[(2\epsilon_s + 1)^2 T]$.
[e] iPrOH is isopropanol and *n*-PrOH is *n*-propanol.

(larger friction) in the excited state, one might imagine that the excited electronic state would have more charge localized near the ends of the molecule, increasing the solute/solvent dielectric coupling. This analysis would be an important test of the validity of the model. However, the modeling of the wave vector dependent dielectric constant is crude enough that the excited state slopes fall within the friction values bracketed by $L = 3$ and $L = 4$ in Table VI. So in addition to excited state charge distributions, a more sophisticated model for the wave vector dependence of the dielectric constant may also be required to test this dielectric friction theory using the excited state data.

Nonexponential decays

Another issue not yet addressed is the multiple exponential decays observed for the ground state rotational diffusion of all three solutes in isopropanol (Fig. 6). This nonexponential behavior has not been observed before for these molecules in alcohols, but that is probably a result of the improved signal to noise of this study. Since the decay of $r(t)$ for these solutes in DMSO is single exponential, it is clear that the multiexponential decays observed in isopropanol reflect new dynamics. Whether or not the excited state rotational relaxation is single exponential remains unclear. The excited state decays collected were noisier (2%–5% of peak signal) than the ground state decays (0.5%–2% of peak signal), which could prevent extraction of the true functional form.

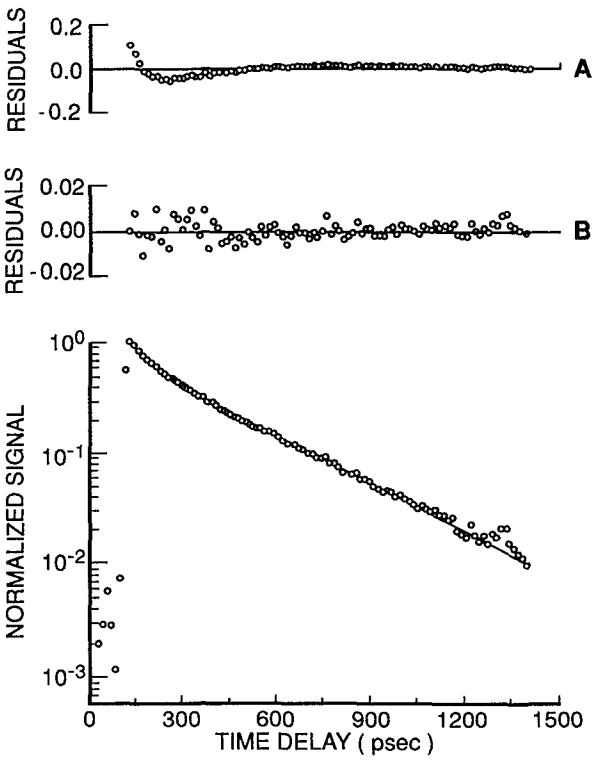

FIG. 6. Ground state decay in isopropanol with residuals for single (A) and double (B) exponential fits.

Two exponential decays have been observed in the past for relatively nonpolar solutes (perylene, dimethylanthracene) in noninteracting solvents.[37] In these systems the friction is mostly hydrodynamic, and the solutes are approximated well by oblate spheroids with the transition moment along a long axis. In this case the full expression for $r(t)$ must be used and accounts for the double exponential decays observed.

In the phenoxazines the friction about the axis along the transition moment is much smaller than the friction about the other two axes, so only one exponential should be observable. Nevertheless, it is actually rather easy to explain this nonexponential behavior, at least in a qualitative way. The formulation of the continuum dielectric friction expressions used thus far have considered solute rotational motion to occur much more slowly than the solvent dielectric relaxation. This limit is appropriate for DMSO ($\tau_D = 20$ ps at room temperature), but not for isopropanol ($\tau_D = 360$ ps at room temperature). In isopropanol it is clear that the frequency dependent dielectric friction coefficient should be used to model the relaxation, which leads to a frequency dependent diffusion constant. The solution of the diffusion equation with frequency dependent diffusion constants yields temporal solutions which are not single exponential decays.

The Hubbard–Wolynes theory,[30] in which a rotational Smoluchowski equation is solved for the solute rotating within the dielectric, provides an alternative mathematical route toward the explanation of such nonexponential behavior. Although solved for a point dipole rotating in the presence of randomly fluctuating torques, the theory could be generalized for an arbitrary distribution of charges. The expression for the friction would reduce to the Eq. (10) when the torque fluctuations occur on time scales faster than the rotation of the solute, resulting in a single exponential decay. This limit is not attained in alcohols, where the torque fluctuations and solute rotation occur on similar time scales. In this case the theory predicts nonexponential behavior, which is indeed observed.

Alternatively, some specific solute/solvent interactions could be used to account for this nonexponential behavior. Two separate populations of dye molecules may exist in solution, some of which are hydrogen bonded and rotate more slowly, and others which are rotating more freely between the hydrogen bonded complexes of solvent molecules. A multiexponential decay could arise from different characteristic decay times for these distinct populations of solute molecules. A preliminary wavelength study revealed no change in the functional form or the decay times with the pump or probe wavelengths. If the different populations had different absorption profiles such a wavelength dependence should be present. Although unlikely, it may be that the different populations have similar spectra and hence no wavelength dependence was observed.

Another mechanism which might produce multiexponential decays is restricted rotational diffusion.[38] If the solute molecule were incorporated into some kind of hydrogen bonded molecular aggregate, one could easily imagine that some solute motions might be more hindered than others. If this were the case, it has been shown that the resulting expression for $r(t)$ would be a multiexponential decay.

Studies are underway to examine the origin of nonexponentiality in these systems.

OXAZINE IN BINARY SOLVENT MIXTURES

The L dependent dielectric friction model can also be used to quantitatively account for the rotational relaxation of oxazine in binary solvent mixtures. The ground state charge distribution was used for this calculation despite the fact that these were excited state measurements, since it was the only charge distribution available. However, in isopropanol oxazine had the weakest state dependence of all the three solutes studied, with the slopes in Table V changing by about 25%. The calculation based on the ground state distribution should still account for the variation of the dielectric friction between the different solvents. Equation (10) was used to calculate the dielectric friction using the cavity radius of 6.70 Å found previously for oxazine in DMSO and varying L_{max} to bracket the experimental slopes. The results of this procedure are given in Table VI. The L_{max} required to reproduce the experimental slopes varied monotonically for the water/alcohol mixtures, from $L = 3$ in pure propanol to $L = 16$–17 for pure water. In contrast, L_{max} does not vary monotonically between pure water and pure DMSO. Starting from pure water ($L = 16$–17), the maximum L decreases to 11–14 for the two water/DMSO mixtures, and then increases to 25 for pure DMSO.

DMSO and alcohols have fundamentally different dielectric relaxation behavior. DMSO relaxes by reorientation of single molecules, while the relaxation of alcohols is dominated by the dynamics of large hydrogen bonded aggregates. Water is also a hydrogen bonded liquid, so its relaxation behavior will also be dominated by multimolecular complexes. As the composition of a mixture is changed from pure propanol to pure water, the basic character of the solvent does not change, but the average size of the transient hydrogen bonded domains in the fluid decreases. This is evident in Fig. 7(a) which shows the dielectric properties of the solvent changing monotonically as the solvent is changed from propanol to water.[39] The characteristic domains are the largest in propanol ($L = 3$) and decrease in size monotonically as the water concentration increases, and are the smallest for pure water ($L = 16$–17). The changing dielectric friction for oxazine in these mixtures reflects the changing size of the domains.

In water/DMSO mixtures the variation in dielectric constant is monotonic as the composition changes from pure DMSO to pure water, but the dielectric relaxation time goes through a maximum at intermediate DMSO concentrations [Fig. 7(b)].[40] What is the physical basis of this variation? Water and DMSO interact strongly, primarily through hydrogen bonding between the DMSO oxygen atom and a water molecule.[41] Pure water, has multimolecular domains of a given size (which yields $L_{max} = 16$–17). Addition of DMSO increases domain sizes as the larger DMSO molecules are incorporated into the water domains. This structure making can explain both the larger relaxation times for wa-

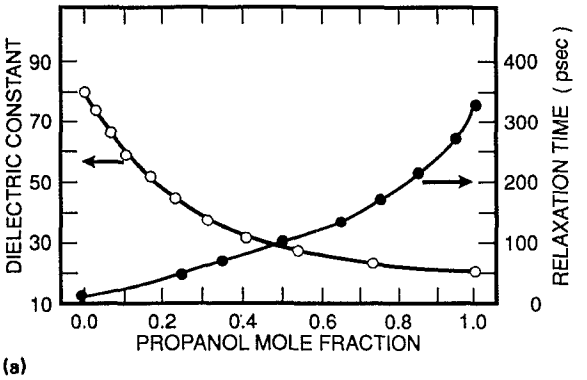

FIG. 7. Dielectric constant and relaxation time for binary solvent mixtures at room temperature. (a) *n*-propanol/water, (b) DMSO/water. Data is taken from Refs. 39 and 40.

ter/DMSO mixtures and also the smaller L_{max} ($L_{max} = 11$–12) required to reproduce the experimental data. As the DMSO concentration is increased further, the amount of DMSO present eventually exceeds the amount which can be accommodated into the domains, and the dielectric relaxation begins to reflect the behavior of single DMSO molecules. The domain size begins to decrease, and L_{max} begins to increase ($L_{max} = 13$–14). Finally, as the limit of pure DMSO is approached, the fast relaxation and large L_{max} ($L_{max} = 25$) characteristic of individual dipolar molecules is reflected in the dielectric relaxation and rotational diffusion data.

As seen previously with pure DMSO and pure isopropanol, the wave vector dependent theory for a general charge distribution can explain the experimental data observed in binary solvent mixtures. It seems clear that a sufficiently rigorous treatment of both the solute electrical properties and the solvent dielectric properties allows successful modeling of experimental data for these phenoxazine dyes in a wide range of different polar solvents. As pointed out earlier for the pure solvents, an alternative explanation for these data in terms of specific solute/solvent interactions could be made. As the solvent composition changes, perhaps the local environment, or solvation shell, would change in a way which altered the solute/solvent coupling. However, the general dielectric friction theory formulated and applied here is able to explain the data presented, and would seem to be a significant first step toward understanding rotational relaxation of solvent molecules in polar solvents.

CONCLUSIONS

The rotational diffusion of the phenoxazine dyes resorufin (anionic), resorufamine (neutral), and oxazine (cationic) was studied in pure DMSO, pure isopropanol, and binary solvent mixtures (DMSO/water and *n*-propanol/water) as a function of temperature. The data were then interpreted in terms of various models of rotational dielectric friction.

In DMSO the rotational relaxation was very different for each of the three solutes, which cannot be explained in terms of hydrodynamics alone. Resorufin reoriented fastest, followed by resorufamine, and then oxazine. The application of the point dipole theories, including the semiempirical theory, to these data yielded dipole moments 5–10 times larger than estimates of the dipole moments made from steady state spectroscopy and electronic structure calculations. This indicated that the point dipole theories underestimate the friction for these molecules by a factor of 100 or more. Only the extended charge distribution model for the dielectric friction expression could yield the correct friction. For pure DMSO L_{max} was 25, since the dielectric behavior of DMSO is mainly determined by the motions of single dipolar molecules.

In isopropanol the results were somewhat different. The relative order of the three dyes in their ground states was different from DMSO, with resorufamine fastest, resorufin next, and oxazine slowest. Once again the point dipole models underestimated the dielectric friction, albeit less severely than in DMSO. Application of the charge distribution theory (without accounting for wave vector dependent dielectric properties) resulted in a friction coefficient that was much too large, and did not reproduce the order of the solute relaxation rates. The key here was to account for the wave vector dependence of the dielectric response of the isopropanol solvent, which forms large hydrogen bonded complexes. Cutting off the series in the general dielectric friction expression at $L_{max} = 3$–4 bracketed the experimentally measured friction, and accounted for the different ordering of the rotation times in isopropanol as opposed to DMSO. Resorufin does not have its outermost charges as close to the boundary as the other two solutes, so truncation of the series [Eq. (10)] at some small L reduces the friction more for oxazine or resorufamine than for resorufin.

Nonexponential decays were observed for these solutes in isopropanol, and could be accounted for qualitatively in several ways. The most obvious is to note that the dielectric friction expressions used in the analyses were obtained in the limit of zero frequency, i.e., assuming the solvent dielectric relaxation was much faster than the solute reorientation. But this limit does not obtain in isopropanol, and use of the full

expression for the frequency dependent friction coefficient, which produces nonexponential behavior, should be used. Alternatively, specific solute/solvent interactions (such as hydrogen bonding) or restricted rotational diffusion could account for the observed behavior. Further studies addressing these issues are underway.

The wave vector dependent dielectric friction theory was also quite successful in explaining the reorientation data for oxazine in binary solvent mixtures. The experimentally determined L_{max} increased monotonically from $L = 3$ for pure propanol to $L = 16$–17 for pure water. This trend reflects the decreasing size of hydrogen bonded complexes, and corresponds to the monotonic variation of the dielectric properties with the composition of these mixtures. In water/DMSO mixtures, the variation of L_{max} was not monotonic, rather $L_{max} = 16$–17 for water, $L_{max} = 11$–14 for mixtures, and then $L_{max} = 25$ for pure DMSO. The initial decrease in L_{max} was interpreted as reflecting an initial increase in solvent complex size as larger DMSO molecules are incorporated into the water complexes. As the DMSO concentration is increased further, the complex size begins to decrease, and the friction approaches its value for pure DMSO. The dielectric relaxation time of DMSO/water mixtures as a function of composition is not monotonic, but has a maximum at $X_{DMSO} \approx 0.35$, which corresponded to the composition yielding the minimum L cutoff (hence the largest complexes) in the analysis. The inclusion of a wave vector dependence into the dielectric friction theory seems to reproduce the essential features of these data.

The issue of specific solute/solvent interactions must be addressed. In isopropanol there may be hydrogen bonding between solute and solvent. In the binary solvent mixtures local interactions may change with composition, altering the solute/solvent coupling. However, in pure DMSO, a polar aprotic solvent, it seems clear that the dielectric friction depends on the higher order moments of the solute charge distribution. Any localized interactions contributing to the friction should increase the observed friction. Since an actual reduction in solute/solvent coupling is observed in isopropanol and the binary mixtures, the wave vector dependence of the dielectric constant must come into play in some way similar to that described. Whether the remaining friction rises entirely from dielectric interactions, or is some combination of dielectric and specific interactions is an open question, and warrants further investigation.

The major result of this paper and the ones preceding it[11-14] has been the formulation of a continuum dielectric friction theory for a solute molecule with an arbitrary charge distribution and its ability to explain a wide range of experimentally observed rotation times. The failure of continuum theories in the past has been taken as an indication that they are not appropriate on molecular length scales. Continuum theories can yield very reasonable estimates of dielectric friction on rotating solute molecules in polar liquids, but only if the solute electronic properties are modeled in a sufficiently realistic manner, and only if the frequency and wave vector dependences of the solvent dielectric properties are taken *into account*. Substituting the molecular charge distribution with a point dipole is just too crude an approximation for the theories to yield accurate estimates of the friction. How successful this model will be with other solute molecule functionalities (so far only NH_2 and $=O$ have been analyzed) and with other solvents remains open.

In conclusion, the rotation times for three solutes with varying electrical properties were measured in a variety of polar solvents. The experimental results can be satisfactorily explained in terms of a dielectric friction model which considers the details of the solute charge distribution as well as the frequency and wave vector dependent dielectric properties of the solvent.

ACKNOWLEDGMENTS

This work was supported with funds from the National Science Foundation Grant No. CHE-8613468. D. S. A. acknowledges support of a Mellon Predoctoral Fellowship for academic year 1989-90. We thank M. Creed for assistance with the dye molecule synthesis. We thank J. Brady and M. Turberg for use of the SLM-8000 fluorimeter. We thank K. Jordan, M. Falcetta, and N. Nystrom for their assistance with the GAUSSIAN 88 program.

[1] G. R. Fleming, *Chemical Applications of Ultrafast Spectroscopy* (Oxford, New York, 1986).
[2] H. E. Lessing and A. von Jena, *Laser Handbook*, Vol. 3, edited by M. L. Stich (North Holland, New York, 1979).
[3] J. L. Dote, D. Kivelson, and R. N. Schwartz, J. Phys. Chem. **85**, 2169 (1981).
[4] (a) D. H. Waldeck and G. R. Fleming, J. Phys. Chem. **85**, 2614 (1981); (b) P. E. Zinsli, Chem. Phys. **20**, 299 (1977); (c) I. Artaki and J. Jonas, J. Chem. Phys. **82**, 3360 (1985); (d) L. A. Phillips, S. P. Webb, and J. H. Clark, *ibid.* **83**, 5810 (1985); (e) K. G. Spears and K. M. Steinmetz, J. Phys. Chem. **89**, 3623 (1985).
[5] (a) J. O'Dell and B. Berne, J. Chem. Phys. **63**, 2376 (1975); (b) J. T. Hynes, R. Kapral, and M. Weinberg, Chem. Phys. Lett. **47** 575 (1977); (c) R. Zwanzig, J. Chem. Phys. **68**, 4325 (1978).
[6] (a) D. Ben-Amotz and T. W. Scott, J. Chem. Phys. **87**, 3739 (1987); (b) D. Ben-Amotz and J. M. Drake, *ibid.* **89**, 1019 (1988).
[7] J. D. Simon and P. A. Thompson, J. Chem. Phys. **92**, 2891 (1990).
[8] D. Kivelson and K. G. Spears, J. Phys. Chem. **89**, 1999 (1985).
[9] (a) G. J. Blanchard, J. Phys. Chem. **92**, 6303 (1988); (b) G. J. Blanchard, J. Chem. Phys. **87**, 6802 (1987); (c) G. J. Blanchard and C. A. Cihal, J. Phys. Chem. **92**, 5950 (1988); (d) G. J. Blanchard, Anal. Chem. **61**, 2394 (1989).
[10] (a) E. F. Gudgin Templeton and G. A. Kenney-Wallace, J. Phys. Chem. **90**, 2896 (1986); (b) **90**, 5441 (1986); (c) E. F. Gudgin Templeton, E. L. Quitevis, and G. A. Kenney-Wallace, *ibid.* **89**, 3238 (1985).
[11] D. S. Alavi, R. S. Hartman, and D. H. Waldeck, *Ultrafast Phenomena VII*, edited by E. Ippen *et al.* (Springer, New York, 1990).
[12] D. S. Alavi, R. S. Hartman, and D. H. Waldeck, J. Chem. Phys. **94**, 4509 (1991).
[13] D. S. Alavi and D. H. Waldeck, J. Chem. Phys. **94**, 6196 (1991).
[14] D. S. Alavi and D. H. Waldeck, J. Phys. Chem. **95**, 4848 (1991).
[15] D. S. Alavi, Ph.D. dissertation, University of Pittsburgh, 1990.
[16] D. S. Alavi, R. S. Hartman, and D. H. Waldeck, J. Chem. Phys. **92**, 4055 (1990).
[17] A. Bondi, J. Phys. Chem. **68**, 441 (1964).
[18] G. K. Youngren and A. Acrivos, J. Chem. Phys. **63**, 3846 (1975).
[19] (a) F. Kehrman und A. Saager, Ber. **36**, 475 (1903); (b) H. Musso and P. Wager, Chem. Ber. **94**, 2551 (1961); (c) D. S. Creed, N. C. Fawcett, and R. L. Thompson, J. Chem. Soc. London, Chem. Comm. **10**, 497 (1981).
[20] (a) V. Stuzka, A. P. Golovina, and I. P. Alimarin, Coll. Czech. Chem. Comm. **34**, 221 (1969); (b) V. Stuzka and E. Sindelarova, *ibid.* **42**, 1332 (1977).
[21] M. J. Frisch, M. Head-Gordon, H. B. Schlegel, K. Raghavachari, J. S. Binkley C. Gonzalez, D. J. Defrees, D. J. Fox, R. A. Whiteside, R. Seeger, C. F. Melius, J. Baker, P. Stewart, E. M. Fluder, S. Topiol, and J. A. Pople, GAUSSIAN 88 (Gaussian, Pittsburgh, 1988).

[22] G. van der Zwan and J. T. Hynes, J. Phys. Chem. **89**, 4181 (1985).
[23] (a) *International Critical Tables*, Vol. VII. (Maple, York, 1930); (b) N. Koizumi and T. Hanai, Bull. Inst. Chem. Res., Kyoto Univ. **33**, 14 (1955); (c) T. Shinomiya, Bull. Chem. Soc. Jpn. **62**, 908 (1985).
[24] A. Einstein, *Investigations on the Theory of Brownian Motion* (Dover, New York, 1956).
[25] F. Perrin, J. Phys. Radium. **5**, 497 (1934).
[26] C. M. Hu and R. Zwanzig, J. Chem. Phys. **60**, 4363 (1974).
[27] E. W. Small and C. Isenberg, Biopolymers **16**, 1907 (1977).
[28] (a) R. Peralta-Fabi and R. Zwanzig, J. Chem. Phys. **70**, 504 (1979); (b) **78**, 2525 (1983).
[29] T. W. Nee and R. Zwanzig, J. Chem. Phys. **52**, 6353 (1983).
[30] J. B. Hubbard and P. G. Wolynes, J. Chem. Phys. **69**, 998 (1978).
[31] (a) J. B. Hubbard, J. Chem. Phys. **69**, 1007 (1978); (b) B. U. Felderhof, Mol. Phys. **48**, 1269 (1983); (c) E. Nowak, J. Chem. Phys. **79**, 976 (1983); (d) B. U. Felderhof, Mol. Phys. **48**, 1283 (1983); (e) P. G. Wolynes, Ann. Rev. Phys. Chem. **31**, 345 (1980); (f) P. Madden and D. Kivelson, J. Phys. Chem. **86**, 4244 (1982).
[32] (a) S. Hyodo, U. Nagashima, and T. Fujiyama, Bull. Chem. Soc. Jpn. **56**, 1041 (1983); (b) P. G. Wolynes, J. Chem. Phys. **68**, 473 (1978); (c) D. Fennel Evans, T. Tominaga, J. B. Hubbard, and P. G. Wolynes, J. Phys. Chem. **83**, 2669 (1979); (d) P. Colonomos and P. G. Wolynes, J. Chem. Phys. **71**, 2644 (1979).
[33] (a) E. W. Castner, G. R. Fleming, B. Bagchi, and M. Maroncelli, J. Chem. Phys. **89**, 3519 (1988); (b) E. W. Castner, G. R. Fleming, and B. Bagchi, Chem. Phys. Lett. **143**, 270 (1988); (c) C. F. Chapman, R. S. Fee, and M. Maroncelli, J. Phys. Chem. **94**, 4929 (1990); (d) P. F. Barbara, Acc. Chem. Res. **21**, 195 (1988); (e) J. D. Simon, *ibid.* **21**, 128 (1988); (f) A. Mokhtari, J. Chesnoy, and A. Laubereau, Chem. Phys. Lett. **155**, 593 (1989).
[34] C. F. J. Böttcher, *Theory of Electric Polarization* (Elsevier, New York, 1973).
[35] (a) R. Minami, K. Itoh, H. Takahashi, and K. Higasi, J. Chem. Phys. **73**, 3396 (1980); (b) H. Mandal, D. G. Frood, M. Habibullah, L. Humeniuk, and S. Walker, J. Chem. Soc. Faraday Trans. 1 **85**, 3045 (1989); (c) J. Barthel, K. Bachhuber, R. Buchner, and H. Hetzenauer, Chem. Phys. Lett. **165**, 369 (1990).
[36] M. Matsumoto and K. E. Gubbins, J. Chem. Phys. **93**, 1981 (1990).
[37] (a) R. L. Christensen, R. C. Drake, and D. Phillips, J. Phys. Chem. **90**, 5960 (1986); (b) M. D. Barkley, A. A. Kowalczyk, and L. Brand, J. Chem. Phys. **75**, 3581 (1981); (c) J. L. Viovy, J. Phys. Chem. **89**, 5465 (1985); (d) H. Labhart and E. R. Pantke, Chem. Phys. Lett. **23**, 482 (1973).
[38] (a) J. M. Schurr, Chem. Phys. **65**, 417 (1982); (b) A. Szabo, J. Chem. Phys. **81**, 150 (1984).
[39] D. Bertolini, M. Cassettari, and G. Salvetti, J. Chem. Phys. **78**, 365 (1983).
[40] Y. Y. Akhadov, *Dielectric Properties of Binary Solutions* (Pergamon, New York, 1980).
[41] (a) F. Franks, *Water: A Comprehensive Treatise* (Plenum, New York, 1973); (b) G. Brink and M. Falf, J. Mol. Struct. **5**, 27 (1970); (c) G. E. Walrafen, J. Chem. Phys. **52**, 4176 (1970); (d) F. Rallo, F. Rodante, and P. Silvestroni, Thermochim. Acta **1**, 311 (1970); (e) R. H. Stokes and R. A. Robinson, J. Phys. Chem. **70**, 2126 (1966).